

RESEARCH PAPER

Synthesized Bimetallic Electrocatalyst for Oxygen Reduction Reaction in Polymer Electrolyte Fuel Cells

Masoumeh Javaheri^{1*}, Maryam Saeidifar², Sara Banijamali¹, Sasan Ghashghaie¹, Marjan Rafiee³

¹ Ceramic Department, Materials and Energy Research Center, Karaj, Iran

² Nano Technology and Advanced Materials, Materials and Energy Research Center, Karaj, Iran

³ Department of Chemistry, Payame Noor University, Tehran, Iran

ARTICLE INFO

Article History:

Received 22 January 2018

Accepted 17 March 2018

Published 01 July 2018

Keywords:

Bimetallic

Oxygen Reduction Reaction

Polymer Electrolyte Fuel Cell

Pt

Ru

ABSTRACT

In the present study, a step by step process was applied to synthesize bimetallic electrocatalyst (Ru and Pt on VulcanXC-72R). This process can reduce the amount of platinum and increase the gas diffusion electrode (GDE) performance in the cathodic reaction of polymer electrolyte membrane fuel cells (PEMFCs). Using the impregnation by hydrothermal synthesis method, a series of electrocatalysts with different molar ratios of metals (Pt and Ru) were prepared and applied in the electrode fabrication process. The performance of the electrodes in Oxygen Reduction Reaction (ORR) was studied using electrochemical methods such as, linear sweep voltametry (LSV), electrochemical impedance spectroscopy (EIS), chronoamperometry techniques, and the membrane electrode assembly (MEA). Also, inductive coupled plasma (ICP), X-ray diffraction (XRD), and transmission electron microscopy (TEM) were employed to characterize the synthesized electrocatalysts. The obtained results indicated that the electrocatalyst with 1:1 molar ratio for Pt:Ru enhanced the cathode performance. This can be attributed to the positive effect of Ru on electronic properties of Pt along with the effect of catalyst distribution on the substrate which consequently provides the best three-phase zones.

How to cite this article

Javaheri M, Saeidifar M, Banijamali S, Ghashghaie S, Rafiee M. Synthesized Bimetallic Electrocatalyst for Oxygen Reduction Reaction in Polymer Electrolyte Fuel Cells. J Nanostruct, 2018; 8(3): 294-299. DOI: 10.22052/JNS.2018.03.009

INTRODUCTION

Platinum has a wide range of catalysis applications due to its unique chemical and physical characteristics [1-5]. The major challenge in this field at present is to reduce the fuel cell energy cost by developing low cost materials, processes, and components [6]. Pt-Metal (Pt-M) bimetallic catalysts are important for their applications in fuel cells. In order to take advantage of Pt-M systems in the design of new catalysts for application in fuel cells, the structural, chemical, and electronic modifications brought about by the addition of secondary metals need to be fully understood. Most emerging approaches focus on controlling the surface structure and composition

of catalytic nanoparticles to achieve higher ORR activity with less Pt and new synthetic routes have been delivered. Recent efforts to improve the performance of Pt-based catalysts have focused on controlling the composition, size, and shape of the catalysts. In reference to fuel cells, alloying Pt with metals such as Fe, Ru, Ni, Co, and other metals has been reported to enhance the oxygen reduction reaction (ORR), increase activity, and enhance resistance to CO poisoning [7-9].

Most studies refer to the catalytic activity of Ru on ORR, but fewer on Pt, in acid or alkaline electrolyte [10,11]. Theoretical and experimental research represented the positive effect of Ru on the electronic

* Corresponding Author Email: m.javaheri@merc.ac.ir

properties of Pt and consequent enhancement of the Pt activity for ORR [12, 13]. The alloy or core-shell structure of Pt and Ru was used for hydrocarbon oxidation (methanol, ethanol and formic acid). The Cu@Pt-Ru was synthesized and used to methanol and ethanol electro-oxidation [14]. The Ru@Pt/Ti₄O₇ [15] had good performance in the presence of CO. The Ru@Pt_x-Pd_y/C were synthesized and applied for formic acid oxidation. [10].

In the other words, because of electron transfer from Ru to Pt, the Fermi level will shift to energy levels higher than pure Pt [16] and the oxygen absorption on Pt can be improved. In addition, the presence of Ru will improve the chemical properties of Pt, directly affecting the adsorption and reduction of oxygen on Pt catalyst [12, 13].

In the present study, regarding the positive effect of Ru on electronic property of Pt, the Pt-Ru/C bimetallic electrocatalyst was synthesis (step by step) by using the impregnation and hydrothermal method to be applied in ORR. The electrocatalysts were characterized by physical and electrochemical techniques.

MATERIALS AND METHODS

Catalyst synthesis

The catalyst was synthesized by a successive reduction route. First, Vulcan powders were pretreated by acidic solution for 12 h. Dispersion of the bimetallic catalyst was carried out using step by step process. In the first step, Ru seeds were dispersed on Vulcan powder. To prepare Ru/C, the RuCl₃·3H₂O precursor in HCl was mixed with Vulcan and was allowed to evaporate in 70°C. Finally, in order to complete the reduction of Ru on Vulcan, the powder was heated in furnace at 200°C under H₂ atmosphere.

To prepare Pt-Ru/C, appropriate amounts of H₂PtCl₆·6H₂O with sodium citrate were dissolved in ethylene glycol and stirred for 1 h. Subsequently, the synthesized Ru/C was added to the mixture and the pH was adjusted up to 10 by drop-wise addition of KOH in ethylene glycol. The mixture was then transferred into a Teflon-lined autoclave and conditioned at 130 °C for 6 h followed by centrifuging, washing, and drying [10]. The molar ratio of Pt:Ru was 1:1, 2:1 and 3:1 in these synthesized catalysts.

Electrode fabrication for three electrode cell and MEA

Three layers of the electrode including carbon paper (substrate), micro porous layer (MPL),

and catalyst layer were fabricated. For MPL, a mixture consisting of 30 wt% PTFE and 70 wt% of VulcanXC72R and in 2-propanol (Merck), water, and glycerol (Merck) was sonicated for 20 min to prepare a homogeneous suspension. The suspension was then rolled onto a teflonized carbon paper TGPH-060T (Toray). The fabricated electrode was finally dried in air at 120°C for 1 h and sintered in air at 340°C for 30 min. To prepare the catalyst layer, a homogeneous suspension was produced from desired amounts of the synthesized electrocatalyst, glycerol (Merck), 2-propanol (Merck), water, and Nafion solution (5% from Aldrich) by using a sonicator for 20 min. The prepared suspension was then rolled onto the diffusion layer. Finally, the electrode containing catalyst loadings of 0.3 mg /cm² was dried at 70°C for 30 min and then at 120° C for 30 min. The same method was used to prepare the cathode and anode of MEA. Of course, for anode fabrication the commercial Pt/C was used [17].

Material characterization

X-ray diffraction (XRD) patterns of the catalysts were recorded by Philips pw 3710, using filtered Cu K_α radiation at 40 kV and 40 mA. The 2θ angles were scanned from 20° to 90°. The morphology of the catalysts was analyzed via transmission electron microscope (CM Philips 30). Also, atomic ratio of metals was determined using the ICP technique (ICP-AES, 314, Switz).

Electrochemical evaluation

An electrochemical potential state (EG&G 2273) was used for the electrochemical measurements. The performance of the porous GDEs (geometric exposed area of 1 cm²) in the reduction of oxygen was investigated in 0.5 M H₂SO₄. All measurements were performed at 25°C in a conventional three-electrode cell with O₂ flowing at 50 mL min⁻¹. The GDEs were mounted into a Teflon holder which contained a graphite disk as current collector, while oxygen feeding was provided from the back of the working electrode. For electrochemical tests, a flat large area platinum electrode was used as the counter electrode and an Ag/AgCl reference electrode was placed close to the working electrode surface. Argon gas was purged into a 0.5 M H₂SO₄ solution during cyclic voltammetry test. All MEA experiments were conducted on a fuel cell test station (Scribner, 850e) where pure and fully humidified hydrogen was used in the anode

Table 1. Name and molar ratio of synthesized catalyst

Catalyst No.	1	2	3
name	11	21	31
Pt:Ru	1:1	2:1	3:1
precursor	%Pt	50	66.5
	%Ru	50	33.5
	%Pt	56	67.9
ICP	%Pt	44	32.1
	%Ru	44	22.2

side, while pure and 50% humidified oxygen was used in cathode side (for reducing the flooding phenomenon). MEA test conditions including the cell temperature of 80°C and cathode and anode gas flow of 200 ml min⁻¹ are presented in Table 1.

RESULTS AND DISCUSSION

The samples contained 7wt% of the catalyst material (ICP results, Table 1). In the XRD pattern (Fig. 1) the peak centering at 24.5° for all the catalysts could be ascribed to the carbon support. There were four observable peaks at 2θ angles of ca. 40°, 47°, 68°, and 81° for Pt plates (111), (200), (220), and (311), respectively. The broadening of peaks indicates that the catalyst particles are of nanometer scale (Table 2). The averages size of the

catalyst particles was calculated using the Scherrer equation after background subtraction [17].

If the nanoparticles could be well dispersed on the carbon substrate, the triple phase zone could be expanded and the electrode performance could be improved. In contrast with the commercial Pt/C, the XRD pattern of the synthesized catalyst (Pt-Ru/C) contains a weak peak at around 43°. This peak is related to Ru (101) and gradually became weaker by reducing the amount of Ru. This phenomenon is attributed to the coverage of Ru particles with Pt, [10, 18]. The presence of the Ru (101) peak reveals that Ru has not been alloyed with Pt. In fact, in the case of alloy formation, Ru atoms would enter the fcc structure, while the introduction of Ru into the hcp structure would be eliminated and consequently remove the Ru (101) peak from the XRD pattern [19]. The XRD results also indicate that the presence of Ru has caused a positive shift in the position and a reduction in the d-spacing of the Pt peaks.

The TEM images (Fig. 2A and 2B) indicate the suitable dispersion of catalyst particles on carbon support in catalyst 11. However, the particles

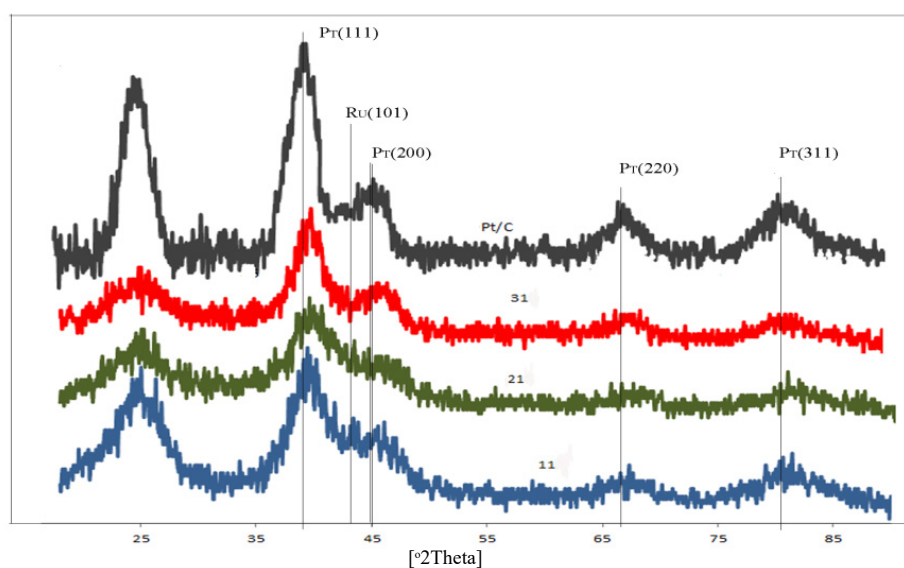


Fig. 1. XRD pattern of catalysts (Ru@Pt) in comparison with commercial Pt/C.

Table 2. Exchange current density, tafel slop, transfer coefficient, current density at 0.3 V, diffusion coefficients, charge transfer resistances, ionic resistances and particle size of all fabricated GDEs

GDE	$i_0 \times 10^{-5}$ (A.cm ⁻²)	b (mV.de ⁻¹)	α_c	i at 0.3(V) (mA.mg ⁻¹)	EAS (m ² .g ⁻¹)	$D^{1/2} \times C^* \times 10^{-8}$ (mol.Cm ⁻² .s ^{-1/2})	R_p (ohm)	d(nm)
11	9.35	42.04	1.41	598.05	27.6	30.69	4.1	2.3
21	4.83	44.35	1.33	447.86	26.54	29.06	4.32	2.1
31	1.26	47.58	1.24	350.86	13.32	16.53	6.75	2.9
Pt/C	7.45	49.12	1.13	461.1	12.7	23	4.73	5

were agglomerated in catalyst 21, reducing the three phase zone and consequently decreasing the electrochemical performance for ORR. These results were also confirmed by electrochemical results (Fig. 3A, 3B, and 3C).

The kinetic parameters of the ORR for a GDE can be obtained from the I-V curve (Fig 3). The analysis of the experimental polarization data was

performed using the Tafel equation [20]:

$$\eta = E - E_{eq} = -b \log \frac{i}{i_0} \quad (1)$$

where, η is the over-potential, E_{eq} is the open-circuit voltage, b is the Tafel slope, i is the current density, and i_0 is the exchange current density for the ORR. The kinetic parameters of the ORR for

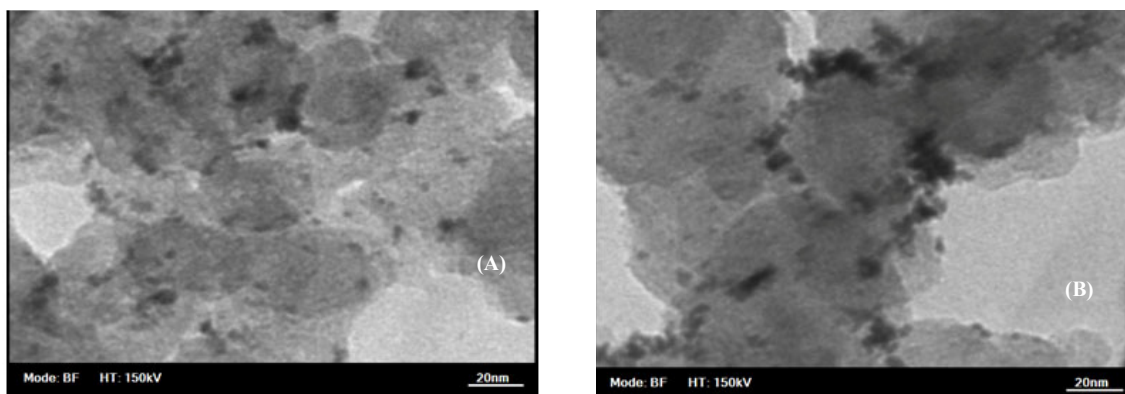


Fig. 2. TEM image of Ru@Pt (A) catalyst 11 (1:1 of Pt:Ru), (B) catalyst 31 (3:1 of Pt:Ru)

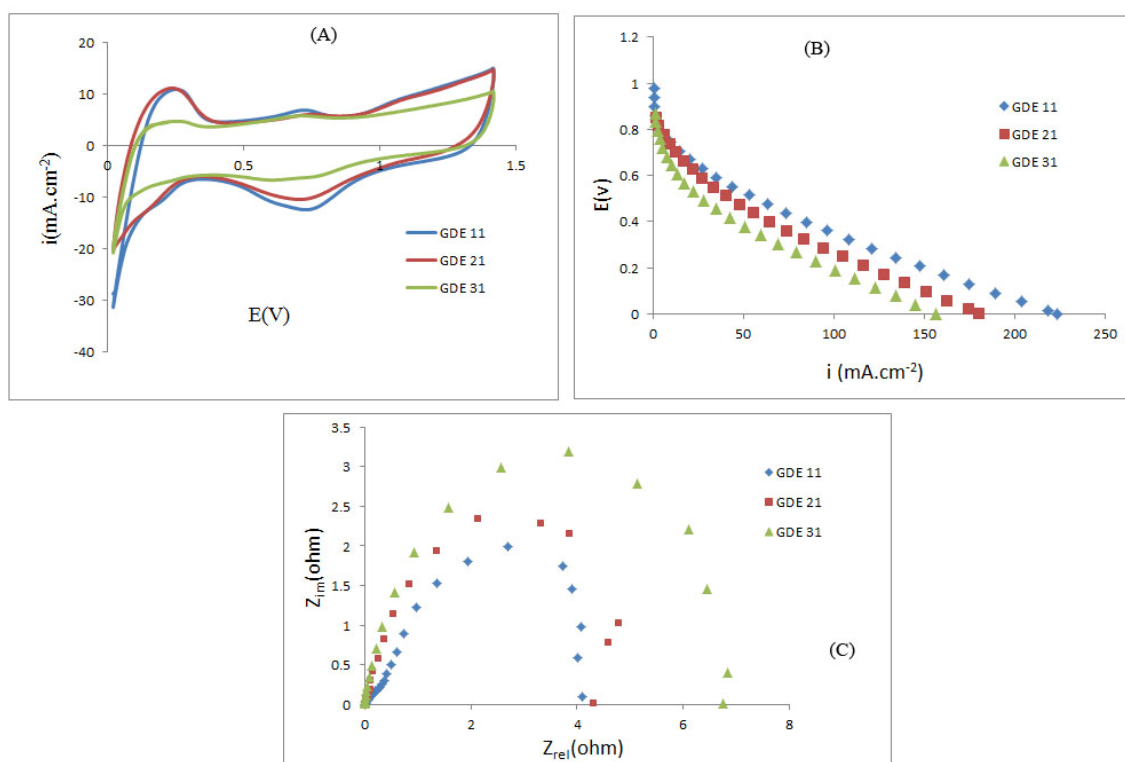


Fig. 3. (A) Cyclic voltammety of electrodes (Ru@Pt) (11◊, 21◻, 31Δ) in 0.5 M H₂SO₄, argon atmosphere, 50 mV.s⁻¹ scan rate and 25°C. (B) LSV curve for electrodes (Ru@Pt) (11◊, 21◻, 31Δ) in 0.5 M H₂SO₄, 5 mV.s⁻¹ scan rate and 25°C. (C) Nyquist plots of the impedance responses from 10kHz to 100mHz for electrodes (Ru@Pt) (11◊, 21◻, 31Δ) in 0.5 M H₂SO₄ at 400 mV and 25°C.

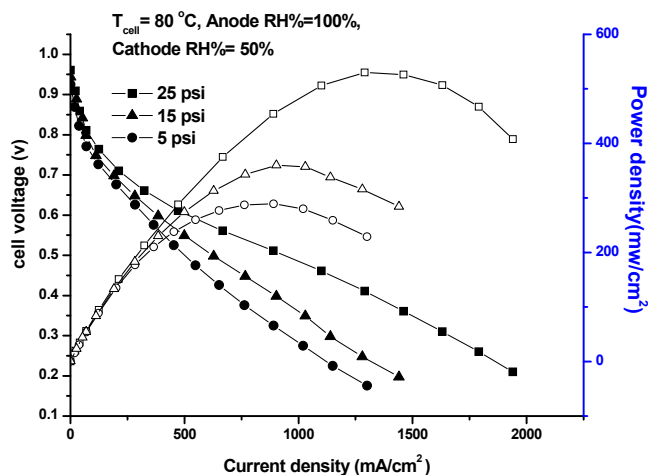


Fig. 4. Polarization curves and power density of catalyst 11(Ru@Pt) in cathode and Pt/C in anode at different gas pressure of 5, 15 and 25 psi, cell temperature 80°C, anode RH=100%, cathode RH=50%.

the GDEs can be obtained from the I-V curves and equation 1.

The exchange current density is an important kinetic parameter which indicated the rate of reaction on the electrode surface. The small Tafel slope at high current density indicates lower activation loss in the polarization curve, revealing a better performance for the electrode (Table 2). The electro active surface area of the electrode was obtained from the cyclic voltammetry results. For this purpose, the coulombic charge for hydrogen desorption was used to calculate the electro active surface area (EAS) of each electrode (Table 2) [21].

Also, using the chronoamperometry experiment and Cottrell equation the diffusion coefficient of oxygen at GDEs can be calculated as follows [22]. It should be emphasized that high diffusion coefficients would result in better accessibility of reactant (Oxygen) and consequently higher performance for ORR.

The higher electrochemical behavior of GDE 11 compared with GDE 21 is attributed to the appropriate dispersion of the catalyst particles in GDE 11 (Fig. 2). It can also be a result of the molar ratio effect and consequently the synergism effect in electrocatalyst 11.

The electrochemical parameters (see Table 2) clearly show that the GDE 11 has the best performance for ORR among all tested catalysts. Closer analysis of the obtained results reveals that the 1:1 molar ratio of Pt:Ru has had the best particle size and catalyst dispersion, enabling it to prepare a better three phase zone than other ratios for ORR.

The MEA was tested using the best synthesized catalyst (11) as cathode and Pt/C as anode. As mentioned in Table 1, the catalyst loading for MEA was 0.3 mg.cm⁻² and the polarization curve was obtained at 3 different gas pressures (5, 15, and 25 psi). The results showed that increasing the gas pressure would increase the performance of MEA (Fig. 4). This could be attributed to the electro catalyst structure and composition which would supply the good diffusion coefficient of oxygen in cathode (Table 2), improving the oxygen reduction reaction. During the membrane electrode assembly testing in O₂, the Pt mass activity was 0.616 A/mgPt at 0.9 V. The voltage at 1 A/cm² was 0.5 V, and a peak power density of 530 mW/cm² was achieved.

The enhanced activity for ORR in catalyst 11 indicated that the step by step process in the synthesis method of Ru and Pt has been able to improve the ORR in PEMFC cathode. The application of this process might lead to a core-shell structure, but unfortunately this idea cannot be proofed due to low quality TEM images taken by our instrument. The good performance in single cell and three-electrode system are attributed to the positive effect of Ru on Pt.

Because of electron transfer from Ru to Pt, the Fermi level will shift to energy levels higher than pure Pt [16] and the oxygen absorption on Pt can be improved. In addition, the presence of Ru in the core will improve the chemical properties of Pt on the shell, directly affecting the adsorption and reduction of oxygen on Pt catalyst [14, 15].

CONCLUSION

In this work, the bimetallic electrocatalyst (Pt-Ru/C) was synthesized using the impregnation and hydrothermal method (step by step process) on Vulcan surface. The application of this process might lead to a core-shell structure. The XRD patterns showed that the synthesized catalyst particles were nano meter-sized.

The result of ICP indicates that this method is suitable for the synthesis of catalyst. Observation of TEM images characterized the dispersion of catalyst on Vulcan substrate. The electrochemical results indicate performance of GDEs for ORR.

The results of physical and electrochemical investigations revealed that the GDE with 1:1 ratio of Pt:Ru has better dispersion, particle size, and performance for ORR than the other catalyst. The MEA results show that this catalyst has good performance on ORR. The maximum power density of this catalyst is 530 mW.cm⁻² at 0.41V.

ACKNOWLEDGEMENT

This work was supported by Materials and Energy Research Center.

CONFLICT OF INTEREST

The authors declare that there is no conflict of interests regarding the publication of this manuscript.

REFERENCES

- Li W-Z, Sun K-Q, Hu Z, Xu B-Q. Characteristics of low platinum Pt-BaO catalysts for NOx storage and reduction. *Catalysis Today*. 2010;153(3-4):103-10.
- Liu P, Wang J, Zhang X, Wei R, Ren X. Catalytic performances of dealuminated H β zeolite supported Pt catalysts doped with Cr in hydroisomerization of n-heptane. *Chemical Engineering Journal*. 2009;148(1):184-90.
- Jahel A, Avenier P, Lacombe S, Olivier-Fourcade J, Jumas J-C. Effect of indium in trimetallic Pt/Al₂O₃SnIn-Cl naphtha-reforming catalysts. *Journal of Catalysis*. 2010;272(2):275-86.
- Matsumoto T, Komatsu T, Arai K, Yamazaki T, Kijima M, Shimizu H, et al. Reduction of Pt usage in fuel cell electrocatalysts with carbon nanotube electrodes. *Chemical Communications*. 2004(7):840.
- Liu Z, Gan LM, Hong L, Chen W, Lee JY. Carbon-supported Pt nanoparticles as catalysts for proton exchange membrane fuel cells. *Journal of Power Sources*. 2005;139(1-2):73-8.
- Moreira J. Synthesis, characterization and application of a Pd/Vulcan and Pd/C catalyst in a PEM fuel cell. *International Journal of Hydrogen Energy*. 2004;29(9):915-20.
- Debe MK. Electrocatalyst approaches and challenges for automotive fuel cells. *Nature*. 2012;486(7401):43-51.
- Kang Y, Murray CB. Synthesis and Electrocatalytic Properties of Cubic Mn-Pt Nanocrystals (Nanocubes). *Journal of the American Chemical Society*. 2010;132(22):7568-9.
- Croy JR, Mostafa S, Hickman L, Heinrich H, Cuenya BR. Bimetallic Pt-Metal catalysts for the decomposition of methanol: Effect of secondary metal on the oxidation state, activity, and selectivity of Pt. *Applied Catalysis A: General*. 2008;350(2):207-16.
- Gao H, Liao S, Zeng J, Xie Y, Dang D. Preparation and characterization of core-shell structured catalysts using Pt_xPd_y as active shell and nano-sized Ru as core for potential direct formic acid fuel cell application. *Electrochimica Acta*. 2011;56(5):2024-30.
- Anastasijević NA, Dimitrijević ZM, Adžić RR. Oxygen reduction on a ruthenium electrode in acid electrolytes. *Electrochimica Acta*. 1986;31(9):1125-30.
- Jakob P, Schlapka A, Gazdzicki P. Oxygen adsorption on Pt/Ru(0001) layers. *The Journal of Chemical Physics*. 2011;134(22):224707.
- Lischka M, Mosch C, Groß A. Tuning catalytic properties of bimetallic surfaces: Oxygen adsorption on pseudomorphic Pt/Ru overlayers. *Electrochimica Acta*. 2007;52(6):2219-28.
- Sieben JM, Comignani V, Alvarez AE, Duarte MME. Synthesis and characterization of Cu core Pt-Ru shell nanoparticles for the electro-oxidation of alcohols. *International Journal of Hydrogen Energy*. 2014;39(16):8667-74.
- Zhang L, Kim J, Zhang J, Nan F, Gauquelin N, Botton GA, et al. Ti₄O₇ supported Ru@Pt core-shell catalyst for CO-tolerance in PEM fuel cell hydrogen oxidation reaction. *Applied Energy*. 2013;103:507-13.
- Kang D. B, Lee C. K. Electronic Properties of Ru/Pt(111) Alloy Surface: A Theoretical Study of H₂O Adsorption. *Bull. Korean Chem. Soc.*, 2000; 21(1): 87- 92.
- Gharibi H, Javaheri M, Kheirmand M, Mirzaie RA. Optimization of the amount of Nafion in multi-walled carbon nanotube/Nafion composites as Pt supports in gas diffusion electrodes for proton exchange membrane fuel cells. *International Journal of Hydrogen Energy*. 2011;36(20):13325-34.
- Zhao H, Li L, Yang J, Zhang Y. Co@Pt-Ru core-shell nanoparticles supported on multiwalled carbon nanotube for methanol oxidation. *Electrochemistry Communications*. 2008;10(10):1527-9.
- Lust E, Härk E, Nerut J, Vaarmets K. Pt and Pt-Ru catalysts for polymer electrolyte fuel cells deposited onto carbide derived carbon supports. *Electrochimica Acta*. 2013;101:130-41.
- Bockris JO'M, *Modern electrochemistry*. Plenum; 2000, 2nd ed: p. 10.
- Pozio A, De Francesco M, Cemmi A, Cardellini F, Giorgi L. Comparison of high surface Pt/C catalysts by cyclic voltammetry. *Journal of Power Sources*. 2002;105(1):13-9.
- Wang J. *Analytical Electrochemistry*. John Wiley & Sons, Inc.; 2000.